Tungsten Oxide Nanopowders and Nanorods Prepared by a Modified Plasma Arc Gas Condensation Technique

C.Y. Su*, Z. K. Yang*, H.C. Lin*, C.K. Lin** and C.H. Chang*
*National Taipei University of Technology, Taipei, Taiwan, R.O.C.
cysu@ntut.edu.tw, s4408014@ntut.edu.tw, s3669018@ntut.edu.tw, s2568034@ntut.edu.tw
**Feng Chia University, Taichung, Taiwan, R.O.C. cklin@fcu.edu.tw

ABSTRACT

In the present study, tungsten oxide nanopowders and nanorods were synthesized by a modified plasma arc gas condensation technique. A blowing mixed gas with controllable partial oxygen pressure was introduced into the gas condensation system and tungsten oxide powders in nanoscale can be prepared. The experimental results show that yellow and blue tungsten oxide nanopowders, prepared under an Ar to O_2 ratio of 1:1 and 100:1, exhibited a major WO_3 and $W_{19}O_{55}$ phase, respectively. The nanoparticles grow into W_5O_{14}-phase nanorods along [001] direction when hydrogen served as the reduction gas.

Keywords: gas condensation, tungsten oxide, nanoparticles, nanorods

1 INTRODUCTION

During the past decades, many efforts have focused on transition metal oxide materials because of their wide applications including electrochromism [1], optics [2], electronics [3], and gas sensors [4]. Among these transition metal oxide materials, tungsten oxide is a promising candidate for the above mentioned applications. Tungsten oxide can exhibit various phases, for instance, stoichiometric WO_2, WO_3, and non-stoichiometric WO_{3-x} ($W_{19}O_{55}$, W_5O_{14} etc.) The phase change of tungsten oxide with respect to temperature has been investigated by Woodward *et al.* [5]. In addition, controlling oxygen concentration can also lead to formation of WO_{3-x} phases ranged from WO_2 to WO_3 [6,7].

With the progress of the nanotechnology, many literatures focus on synthesizing one-dimensional (1D) tungsten oxide nanomaterials, including nanorods [8], nanowires [9], and nanotubes [10]. For instance, Guo *et al.* [11] synthesized nanocrystalline tungsten oxide powders by direct current arc discharge. While Zhu *et al.* [12] produced tree-like WO_3 nanorods by heating a W foil with SiO_2 plate under an argon atmosphere. In addition, $W_{18}O_{49}$ nanowires have also been synthesized by controlling the oxygen content during the sputtering process [13]. In the present study, plasma arc was used as the heat source to evaporate tungsten target. A modified plasma arc gas condensation technique was proposed to prepare tungsten oxide nanopowders or nanorods by controlling atmosphere in the process. Structural properties of the as-prepared nanomaterials were also investigated.

2 EXPERIMENTAL PROCEDURES

Tungsten raw material with a purity of 99.95% (Ample Goal International, Co. LTD, Japan) was heated by a water-cooled plasma gun (model ： PWM-300, Thermadyne International, USA), evaporated in the controlled atmosphere, and collected on the cold trap [14]. The voltage and the current of plasma arc were 20V and 80A, respectively. An inlet gas nozzle placed close to the plasma was used to introduce a mixed gas flow of argon and oxygen with a ratio of 1:1 and 100:1. Dynamic gas pressure equilibrium was maintained carefully at a pressure of 200 torr during the processing. Figure 1 shows the schematic illustration of the modified plasma arc gas condensation system used in the present study. Tungsten oxide nanorods, however, were prepared using the processing parameters of Ar/O_2=100:1 (chamber pressure also fixed at 200 torr), but 10% hydrogen gas was added into the plasma gas.

The as-received nanocrystalline powders and nanorods were characterized by transmission electron microscopy (TEM), X-ray diffraction (XRD), synchrotron x-ray absorption spectroscopy, and field emission gun scanning electron microscope (FEG-SEM). The morphology of as-prepared nanopowders and nanorods was observed by a field emission gun scanning electron microscope (FEG-SEM, Leo 1530, Germany).The particle size, shape and distribution can be obtained from the bright field image of TEM photographs. Meanwhile, detailed structural information was examined by a Phillip Techai 20 high resolution transmission electron microscope (HRTEM, Philips, Tecnai F20, Holland) and an analytical transmission electron microscope equipped with energy dispersive spectrometer (AEM/EDS, JEOL, JEM-2010, Japan). The phase identification of nanocrystalline powders and nanorods were performed using a high power X-ray diffractometer (M21X, MAC Science Co., Ltd) with a monochromatic Cu Kα radiation. Synchrotron X-ray absorption near edge structure (XANES) measurements were performed at the Wiggler-C beam line of the National Synchrotron Radiation Research Center (NSRRC) in Hsinchu, Taiwan. Experiments were performed on as-prepared materials using fluorescence and transmission modes at W L_{III} edge, i.e., 10.2068 keV. A standard W foil was used to calibrate the photon energy before and after the XANE measurements.

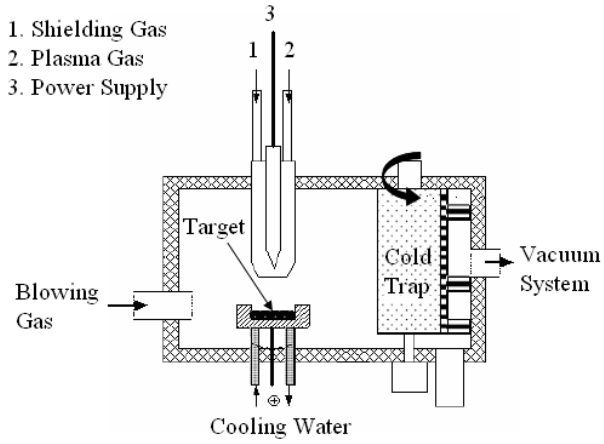

Figure 1: Schematic of plasma arc gas condensation equipment.

3 RESULTS AND DISCUSSION

3.1 Phase Characterization

It is interesting to note that the as-prepared nanocrystalline powders exhibited different colors during the processing. Since tungsten oxide exhibited various stoichiometric (such as WO_2 and WO_3) and nonstoichiometric (WO_{3-x}) compositions, X-ray diffraction was used to examine the phases of the as-prepared nanocrystalline powders. Figure 2 shows the X-ray diffraction patterns of as-obtained tungsten oxides prepared using various processing parameters. It can be noted that yellowish tungsten oxide powders prepared with an Ar/O_2 ratio = 1:1 (curve (a) in Fig. 2) exhibited a stoichiometric WO_3 phase (JCPDS card number: 05-0363). While blue tungsten oxide powders (curve (b), prepared with an Ar/O_2 ratio = 100:1) possessed best-identified $W_{19}O_{55}$ phase (JCPDS No.: 45-0617) and other minor phases. The bluish purple nanocrystalline powders prepared with 10% H_2 added in the Ar plasma gas (curve (c)), however, showed a majority of W_5O_{14} phase (JCPDS No.: 41-0745) with limited minor phase. XRD results indicated that WO_3 phase exhibited if sufficient oxygen was supplied, while non-stoichiometric tungsten oxide powders (for instances $W_{19}O_{55}$ and W_5O_{14}) formed under an oxygen-deficient or hydrogen-supplied reductive environment. In our previous study [14], the spherical tungsten oxide nanopowders turns from the ellipse shape to the rod-like shape when the oxygen partial pressures are changed. Hence, the oxygen defects truly affect the structures of the tungsten oxide nanoparticles

In addition to the X-ray diffraction analysis explored the long range atomic order, synchrotron X-ray absorption near edge structure (XANES) technique reveals the electronic structure of the detected element. Figure 3 shows the XANES spectra of the W L_{III}-edge for the corresponding tungsten oxide powders (i.e., WO_3, WO_{3-x}, and W_5O_{14}) examined by XRD in Fig. 2. It can be noted that the main absorption peak shifted to the right with respect to WO_3, WO_{3-x}, and W_5O_{14}. The main absorption peaks are 10.2115, 10.2099, and 10.2080 keV, respectively. The tungsten valence of the as-prepared WO_3, WO_{3-x} ($W_{19}O_{55}$ as the major phase), and W_5O_{14} powders is +6, +5.8 (calculated from $W_{19}O_{55}$), and +5.6, respectively. The decreasing absorption peak energy confirmed the decreasing oxidation states of tungsten (i.e. valence) in tungsten oxide powders. This shows a similar trend as reported by Khyzhun [15].

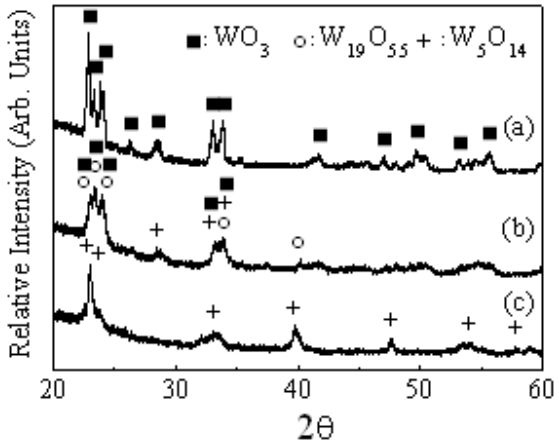

Figure 2 : XRD pattern of various tungsten oxide nano-powders and rods prepared using (a) Ar/O_2=1:1, Ar plasma gas, (b) Ar/O_2=100:1, Ar plasma gas, and (c) Ar/O_2=100:1, Ar+10%H_2 plasma gas.

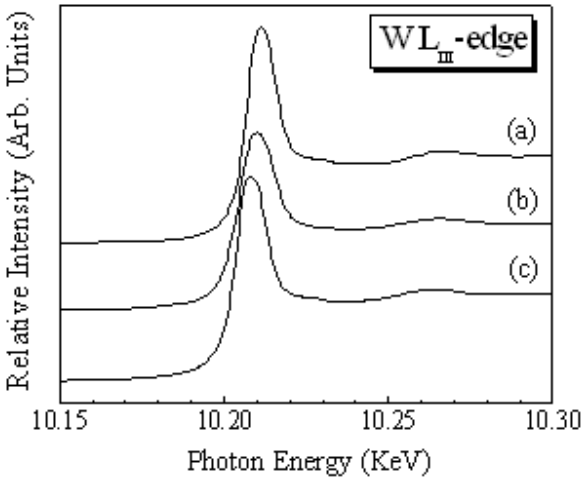

Figure 3 : XANES spectra corresponding to those shown in Fig.2

3.2 Morphology and Structural Investigation

Figure 4 shows the particle morphology of the as-prepared tungsten oxide powders. It can be noted that the

yellowish nanocrystalline WO_3 powders (Fig. 4a) exhibited a relative large grain size as compared to that of blue WO_{3-x} powders (Fig. 4b). The average grain size determined from the TEM images for the as-prepared nanocrystalline WO_3 and WO_{3-x} powders is 28.8 ± 9.8 and 15.8 ± 4.7 nm, respectively. As shown in Fig. 4b, it is interesting to note that a small amount of nanorods were synthesized under an oxygen-deficient environment (Ar/O_2=100:1). Tungsten oxide nanorods, as shown in Fig. 4c, can be observed under a reductive atmosphere where 10% H_2 gas was added into the plasma. The bluish purple W_5O_{14} nanorods exhibited an average diameter of 15.2 ± 5.4 nm with a length ranged from 20 nm to several microns. Since TEM can observe only a small portion of as-prepared powders, an overall picture was investigated by field emission scanning gun electron microscope (FEG-SEM). As shown in Fig. 5, the FEG-SEM image revealed that tungsten oxide nanorods were synthesized successfully as the major product (say over 95%) under a reductive environment.

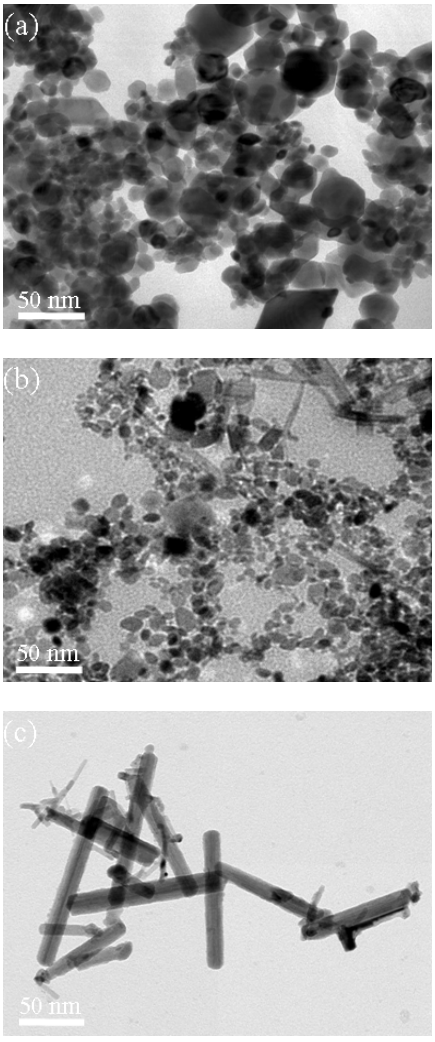

Figure 4 : TEM images of (a) WO_3, (b) WO_{3-x} nanocrystalline powders, and (c) W_5O_{14} nanorods.

It is interesting to note that the bluish purple W_5O_{14} nanorods (as shown in Fig. 4c by TEM and Fig 5 by FEG-SEM) were very straight. In order to further understand the crystallographic orientation of the longitude direction, HRTEM was used to examine the W_5O_{14} nanorods. Figure 6 shows the HRTEM image and the inset is the corresponding electron diffraction pattern, respectively. The longitude direction (also the possible growth direction) of the W_5O_{14} nanorods is [001] and the d-spacing is ~0.38 nm. It is suggested that polyhedral tungsten oxide (either WO_3 or $W_{19}O_{55}$), as prepared with Ar/O_2 ratio from 1:1 to 100:1, exhibited the equi-axed growth mode during the process. While under a reductive atmosphere where 10% H_2 gas was added into the plasma gas, [001] direction became a preferred growth orientation and formed W_5O_{14} nanorods. Though the growth mechanisms for tungsten oxide nanorods have been proposed by various researchers [12,17-19], W_5O_{14} nanorods were first prepared by present plasma arc condensation technique.

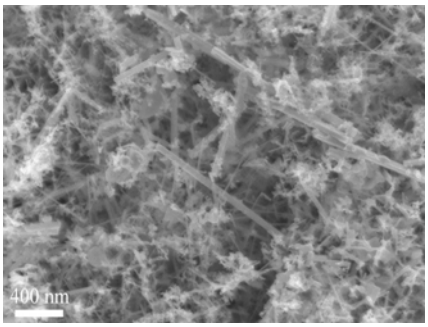

Figure 5 : A FEG-SEM image of as-prepared W_5O_{14} nanorods.

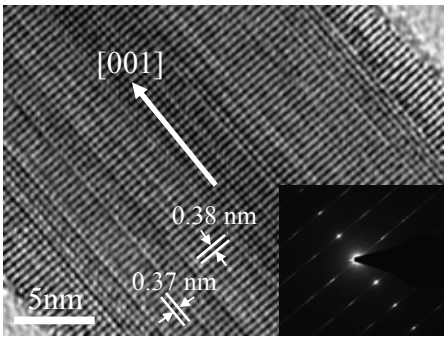

Figure 6 : A HRTEM image of W_5O_{14} nanorods and the inset is the corresponding electron diffraction pattern.

For the discussion of the nanorod growth mechanism , the vapor-liquid-solid (VLS) growth mechanism has been investigated, in which metal nanoparticles acting as the catalyst are found at the tips of the nanorods [20]. Based on the TEM measurements, however, we could not find the essential condition for the VLS growth mechanism. Due to the nucleation and growth mechanism proposed by the gas condensation [21,22], the vapor-solid (VS) growth

mechanism, which has been used for whiskers growth [23,24], may apply to the case in this research. As the tungsten target is evaporated by plasma arc, the tungsten atoms react with the trace oxygen atoms existing at the chamber. Hence, tungsten oxide nanoparticles are formed during the process. Once the hydrogen atoms from the plasma arc react with the tungsten oxide nanoparticles, the nonstoichiometric tungsten oxide nanoparticles are formed. The driving fore induced by plasma arc with high temperature will make W_5O_{14} nanorods grow along the directions of the deficient-oxygen sites and W_5O_{14} nanorods are finally formed. The schematic illustration of W_5O_{14} nanorods synthesized by this technique is shown in Figure 7.

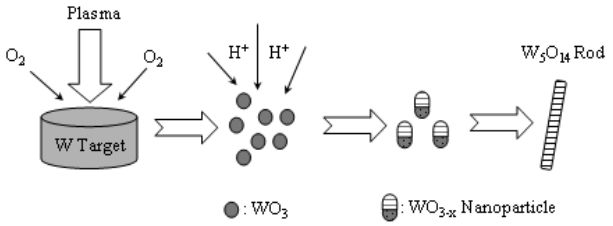

Figure 7 : The illustration of the growth mechanism of W_5O_{14} nanorods synthesized by a modified plasma arc gas condensation.

4 CONCLUSIONS

A modified plasma arc gas condensation technique was used to prepare tungsten oxide nanopowders and nanorods. By controlling the partial oxygen pressure of the mixed gas, yellow WO_3 and blue $W_{19}O_{55}$ tungsten oxide powders (major phase) were prepared under an Ar/O_2 gas ratio of 1:1 and 100:1, respectively. Bluish purple nanorod particles were synthesized by adding 10% hydrogen gas into the plasma. The mean grain size of WO_3 and WO_{3-x} was ~29 and 16 nm, respectively, while bluish purple W_5O_{14} nanorods exhibited an average diameter of 15 nm with various lengths. Polyhedral tungsten oxide (either WO_3 or $W_{19}O_{55}$), as prepared with Ar/O_2 ratio from 1:1 to 100:1, exhibited the equi-axed growth mode during the process. While [001] orientation became the preferred growth direction and W_5O_{14} nanorods formed, if 10% H_2 gas was introduced into the plasma gas.

REFERENCES

[1] C.G. Granqvist, Sol. Energy Mat. Sol. Cell. 60, 201, 2000 .

[2] I. Turyan, U.O. Krasovec, B. Orel, T. Saraidorov, R. Reisfeld and D. Mandler, Adv. Mater. 12, 330, 2000.

[3] E.K.H. Salje, Europ. J. Solid State Inorg. Chem. 31, 805, 1994.

[4] W.M. Qu and W. Wlodarski, Sens. Actuators B 64, 42, 2000.

[5] P.M. Woodward and A.W. Sleight, J. Solid State Chem. 131, 9, 1997.

[6] M.G. Hutchins, N.A. Kamel and K. Abdel-Hady, Vacuum 51, 433, 1998.

[7] S.H. Lee, H.M. Cheong, C.E. Tracy, A. Mascarenhas, A.W. Czanderna and S.K. Deb, Appl. Phys. Lett. 75,1541, 1999.

[8] K. Lee, W.S. Seo and J.T. Park, J. Am. Chem. Soc. 125,3408, 2003.

[9] G. Gu, B. Zheng, W.O. Han, S. Roth and J. Liu, Nano Lett. 2, 849, 2002.

[10] Y. Li, Y. Bando, and D. Golberg, Adv. Mater., 15, 1294, 2003.

[11] Y. Guo, N. Murata, K. Ono and T. Okazaki, J. Nanopart. Res. 7, 101, 2005.

[12] Y.Q. Zhu, W. Hu, W.K. Hsu, M. Terrones, N. Grobert, J.P. Hare, H.W. Kroto, D.R.M. Walton and H. Terrones, Chem. Phys. Lett. 309, 327, 1999.

[13] C.H. Chen, S.J. Wang, R.M. Ko, Y.C. Uang, T.M. Chen, B.W. Liou and H.Y. Tsai, Nanotechnology, 17, 217, 2006

[14] C.Y.Su, C.K.Lin, H.C.Lin, C.H. Chang and P.T. Pan, 2nd International Symposium on Point Defect and Nonstoichiometry, Kaohsiung, Taiwan, 2005.

[15] C.Y. Su, C.K. Lin and C.W. Cheng, Mater. Trans. 6, 1016, 2005.

[16] O. Yu. Khyzhun, J. Alloys Comp. 305, 1, 2000.

[17] Y.B. Li, Y. Bando, D. Golberg and K. Kurashima, Chem. Phys. Lett. 367, 214, 2003.

[18] S. Vaddiraju, H. Chandrasekaran and M.K. Sunkara, J. Am. Chem. Soc. 125, 10792, 2003.

[19] Z. Liu, Y. Bando and C.C. Tang, Chem. Phys. Lett. 372, 179, 2003.

[20] R.S. Wagner and W.C. Ellis, Appl. Phys. Lett. 4, 89, 1964.

[21] H. Gleiter, Prog. Mater. Sci. 33, 223, 1989.

[22] C.Y.Su, H.C. Lin, W. Lin and C.K. Lin, Nanotechnology (in press)

[23] Y.J. Hsu, and S.Y. Lu, J. Phys. Chem. B, 109, 4398, 2005.

[24] A. Sekar, S.H. Kim, A. Umar, and Y.B. Hahn, J. Crystal Growth, 277, 471, 2005.